Journal of Structural Geology, Vol. 15, Nos 3–5, pp. 383 to 390, 1993
Printed in Great Britain

0191-8141/93 $06.00+0.00

Strain and magnetic remanence

GRAHAM JOHN BORRADAILE

Geology Department, Lakehead University, Thunder Bay, Ontario, Canada P7B 5E1

(*Received* 23 *October* 1991; *accepted in revised form* 30 *March* 1992)

Abstract—Experimental data may be compatible with the hypothesis that a single direction of magnetic remanence rotates as a rigid marker with strains up to 40% shortening in coaxial, perfect flattening ($X = Y > Z$). Detailed agreement with the passive line model is relatively poor for the specimens in which remanance is carried by magnetite. However, for this range of strains the differences with the passive line model (Wettstein's equation) are so slight that the latter model may be more easily employed to de-strain or restore deformed remanance to its original attitude. In the case of hematite-bearing remanences, the differences between the passive line and rigid marker model are even smaller because of the higher aspect ratios of grains of hematite. Therefore it is suggested that Wettstein's equation may be safely used to restore remanence after even higher strains, where the remanence is carried by hematite.

INTRODUCTION

THERE has been increasing interest over the last few years in paleomagnetic research of penetratively strained rocks. Traditionally, paleomagnetists have corrected the orientation of the characteristic pre-tectonic remanence vector for the tilt of the enclosing strata and also for the plunges of gentle folds (MacDonald 1980). To some degree, the effects of syn-folding penetrative deformation have been investigated (e.g. van der Pluijm 1987, Kodama 1988, Stamatakos & Kodama 1991) but, generally, penetratively strained rocks such as slates and schists have been avoided in paleomagnetic studies. This is because the method of correcting paleomagnetic remanence directions for the effects of homogeneous strain has remained problematical (Cogné & Gapais 1986, Cogné & Perroud 1987, Borradaile & Mothersill 1989), especially at the grain scale (van der Pluijm 1987, Stamatakos & Kodama 1991). In particular, the non-cummutative nature of successive non-coaxial strains and of successive strains and rotations (Borradaile & Mothersill 1989, fig. 1) makes it impossible to de-strain a tectonite successfully in many situations. However, by assuming homogeneous strain and a coaxial strain history, some researchers have de-strained a single-component remanence direction by hypothesizing that it behaved as a passive line (equation 1 below) during deformation. Workers who have done this include Borradaile in discussion of Tarling (1974), Kligfield *et al.* (1981, 1983), Cogné & Perroud (1985), Hirt *et al.* (1986), Cogné (1987a, 1988) and Lowrie *et al.* (1986). In the studies cited, it has been assumed that whatever model explains the rotation of a characteristic uniform remanence component is also the model that explains the physical rotation of the grains which carry the remanence. This may seem a redundant point, but rock magnetists are well aware that remanence may suffer a permanent rotation as the result of high stresses, with insignificant strain or grain rotation, especially in multi-domainal magnetite (e.g. Nagata 1970). A natural example of progressive rotation of remanence by plastic grain deformation and rotation has been documented by Rosenbaum (1986) in which a welded tuff suffered compaction while still hot but below the blocking temperatures of the remanence-carrying grains.

Initial experimental tests of strain on artificially magnetised samples were hindered by the non-ductile response of most earth materials at room temperature (Kodama & Cox 1978, Pozzi & Aïfa 1989); to some extent experiments with Plasticine (Cogné 1987b) were more instructive. The present author has overcome the problem of limited ductility of most rocks at room temperature by using limestones (Borradaile 1991), a specially selected sandstone with easily compactable, retrogressed feldspars (Borradaile & Mothersill 1989, 1991) and aggregates of mineral grains bonded with Portland cement (Borradaile 1992, in press, Jackson *et al.* in press). These materials all behave in a macroscopically ductile fashion at room temperature, for strains up to about 30% shortening in a perfect flattening deformation (where $X = Y > Z$ are the principal stretches). Greater shortening produces heterogeneous strain in these samples for which the remanence behaviour is more difficult to decipher.

Cylindrical specimens of the materials have been given an isothermal remanent magnetisation in selected directions, jacketed in Teflon tubing, and deformed in a triaxial rig at 200 MPa (2 kbar) confining pressure or in the case of the sandstone at 100 MPa (1 kbar). In some cases a pore fluid pressure was applied at 60 or 80% of the confining pressure in order to reduce the differential stresses during ductile flow. The triaxial rig is controlled by a personal computer which monitors axial load, confining pressure, fluid pressure and piston displacement. The program makes real-time corrections for specimen and pressure vessel distortion and sends a signal to the hydraulic loading pump to control the strain-rate every 27 s. In this way strain-rates are controlled precisely to avoid any jerking that might induce discontinuous failure of the specimens. All the specimens described here were strained at a natural strain-rate of $10^{-5}\,s^{-1}$. A natural strain-rate is one in which the

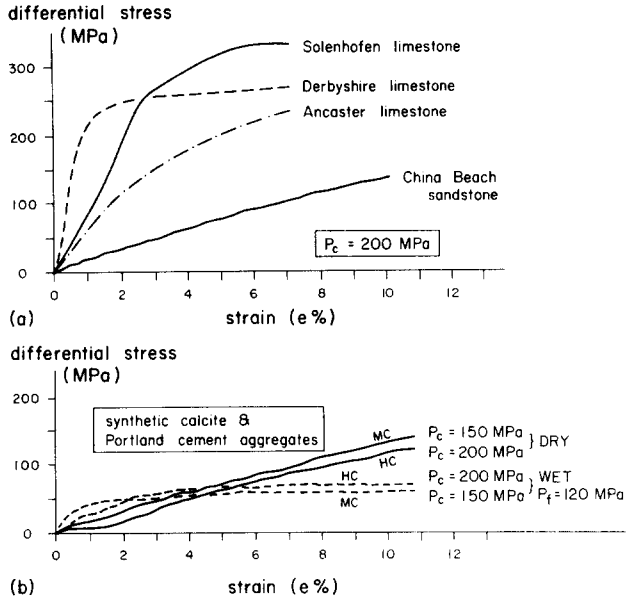

Fig. 1. Stress–strain relations for typical samples of the materials used in the triaxial tests. Pc = confining pressure (σ_3), differential stress = ($\sigma_1 - \sigma_3$), Pf = pore fluid pressure. 100 MPa = 1 kbar. In (b) MC = magnetite–calcite aggregate, HC = hematite–calcite aggregate.

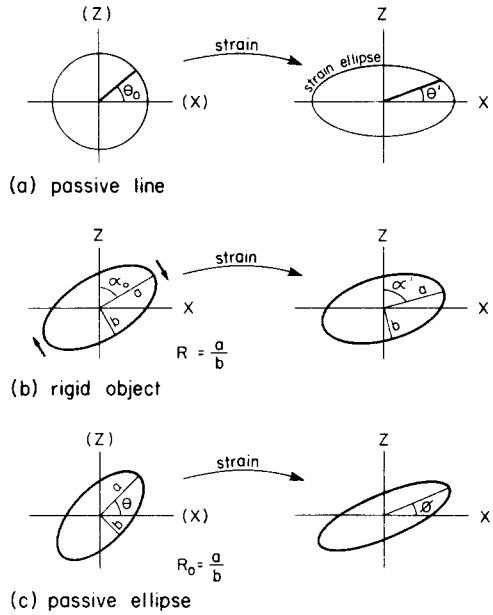

Fig. 2. Angular conventions used in the three models for the reorientation by strain of the long axes of grains carrying magnetic remanence. Note R is constant in the case of rigid rotation but R_0 changes in the case of strain of a passive elliptical marker.

strain is calculated for each increment relative to the current length, rather than the initial length at the start of the experiment (Pfiffner & Ramsay 1982). Further experimental details are given elsewhere (Borradaile & Mothersill 1989, 1991). Typical stress–strain graphs are shown for the experimental materials in Fig. 1.

After deformation the remanence of each specimen was remeasured to determine the effects of strain. It was then progressively demagnetized in an alternating field demagnetizer to investigate the effects of strain on the components of different coercivity that compose the total remanence. Demagnetization was sometimes done immediately after the experimental deformation and, in order to investigate the durability of the strain-induced changes, sometimes at a later date.

Alternating field (a.f.) demagnetization was also necessary to determine if any remagnetization occurred due to the pressure vessel. This is known to have an internal, upwards directed axial field of 31 μT, less than the Earth's magnetic field in the laboratory (Borradaile & Mothersill 1991). Thus the pressure vessel acts as a feeble magnetic shield. Nevertheless, in some materials, a room-temperature deformational viscous remagnetization (Borradaile & Mothersill 1991) imparted a tiny upwards component of magnetization to the specimen. This was responsible for a negligible change in the resultant remanence. It was removed by a few mT a.f. demagnetization so that the true physical rotation of the remanence vector due to strain could be recognized.

THEORY

Rotation of a passive line

The simplest theory that has been applied to the rotation of remanence is that a uniformly oriented remanence vector (in field studies this would be the characteristic component of the natural remanent magnetization) rotates as a passive line according to Wettstein's equation (Ramsay 1967, equation 3-34):

$$\frac{\tan\theta'}{\tan\theta_0} = \frac{1}{R_s}, \qquad (1)$$

where $R_s = X/Z$ is the strain ratio, for principal strains $X \geq Y \geq Z$, with the angular convention shown in Fig. 2.

This formula is valid only for a two-dimensional strain, *pure shear*, in which $X = 1/Z$ and $Y = 1$. Nevertheless, it may be applied in natural situations to projections of a line onto the principal planes of the strain ellipsoid in a more general strain with $X \geq Y \geq Z$ (Ramsay & Huber 1983, p. 177). It is in this manner that previous field studies of strained remanence have restored the remanences to supposed de-strained attitudes. In the present experiments the sample cylinders are shortened axially and extend equally in all directions perpendicular to the axis. Thus the deformation is a *coaxial perfect flattening* in which $X = Y > Z$, and since there is constancy of volume $X \,.\, Y \,.\, Z = 1$, we may write

$$\frac{\tan\theta'}{\tan\theta_0} = Z^{1.5} \qquad (2)$$

for the rotation of the inclination of the initial remanence vector θ_0 with respect to the horizontal for a vertical shortening (Z) of the cylinder axis. This relationship has been applied in previous experimental studies of remanence in the author's laboratory (Borradaile 1991, Borradaile & Mothersill 1991) with some success in explaining the experimental response of the remanence to strain.

However, it is more realistic to expect that the remanence rotates in some manner comparable to the actual strain-response of the particles carrying the remanence

rather than as a passive line (equation 1). Magnetite or hematite commonly carry the remanence in nature and are also the carriers in this experimental study. Such minerals are expected to deform very little in a sedimentary rock deforming at low temperature. Thus, as extreme limiting cases, we may consider the effects of rotation on a rigid object in a passive matrix (Ghosh & Ramberg 1976) and the effects of strain rotation on a passive object which re-shapes itself during strain (Ramsay 1967, Chap. 5, the "R_f/φ Model").

Rotation of the long axis of a rigid marker

For a rigid marker of aspect ratio R (see Fig. 2b for conventions, particularly of the angles) undergoing *pure shear* it is shown that the rate of rotation of the long axis in terms of the rate of extension of the X-direction of the matrix is given by (Ghosh & Ramberg 1976, equation 2):

$$\delta\alpha = \delta\varepsilon_X \cdot \frac{(R^2-1)}{(R^2+1)} \cdot \sin 2\alpha. \tag{3}$$

Note the angular convention (Fig. 2b) $\alpha = 90 - \theta$ and that $\varepsilon_X = \ln(X)$. $R_s = X/Z$ and, for pure shear $X = 1/Z$, thus

$$\varepsilon_X = \tfrac{1}{2}\ln(R_s) \tag{4}$$

and for perfect flattening, as in these experiments, $X^2 = 1/Z$ so

$$\varepsilon_X = \tfrac{1}{3}\ln(R_s). \tag{5}$$

On rearranging and integrating equation (3) we obtain:

$$\int_{\alpha_0}^{\alpha'} \operatorname{cosec} 2\alpha \, d\alpha = \frac{(R^2-1)}{(R^2+1)} \cdot \int_0^{\varepsilon_X} d\varepsilon_X \tag{6}$$

which yields:

$$\frac{1}{2}\ln(\tan\alpha') - \frac{1}{2}\ln(\tan\alpha_0) = \frac{(R^2-1)}{(R^2+1)} \cdot \varepsilon_X. \tag{7}$$

This relates the rotation, from α_0 to α', of the long axis of a rigid marker of constant aspect ratio R to the logarithmic extension ε_X.

Rotation of the long axis of a passive marker

This model has been much used by structural geologists to provide a limiting case for the alignment of passive objects (showing no ductility contrast with their matrix) during homogeneous strain. Considering a passive elliptical marker, Ramsay (1967, Chap. 5) showed that the long axis of an elliptical marker with initial axial ratio R_0 changes aspect ratio during deformation, and its long axis appears to rotate from an angle θ to an angle φ (see Fig. 2c) according to (Ramsay 1967, equation 5-22):

$$\tan 2\varphi = \frac{2R_s \cdot (R_0^2-1) \cdot \sin 2\theta}{(R_0^2+1)(R_s^2-1) + (R_0^2-1)(R_s^2+1) \cdot \cos 2\theta}. \tag{8}$$

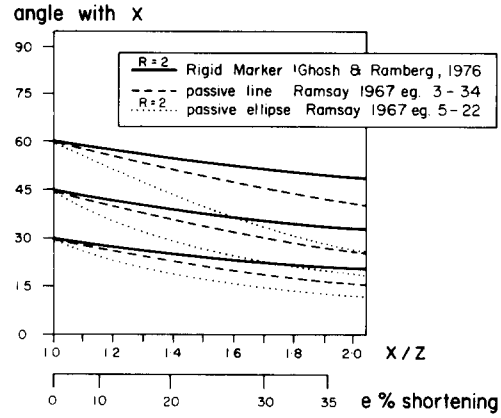

Fig. 3. The rotation of linear elements according to the three models. For the rigid marker model (equation 7) and the passive ellipse model (equation 8), the long axis represents the linear element in question and the ratio of the long axis/short axis is given by $R = 2$ for the curves shown ($R_0 = 2$ for the passive marker which changes ratio during deformation). The passive line model is represented by equation (1). For large values of R and R_0 the three equations converge; in practice at these strains $R = 5$ would be considered large.

Comparison of the three theoretical models

The three models described above are limited in their degree of realism, but they are presented here in order to provide guidelines with which to compare the experimental data.

The three formulae (equations 1, 7 and 8) for the rotation of a passive line, rigid marker and passive elliptical marker for an elementary, two-dimensional, coaxial strain history of *pure shear* are compared in Fig. 3. Clearly under these circumstances, rigid markers rotate most slowly, passive lines more quickly and passive ellipses still more quickly.

The examples shown are for markers of initial long axis to short axis ratios, $R = 2$. As progressively larger values of R are chosen, the rigid marker's rotation becomes faster and the passive marker's rotation becomes slower until, for $R = \infty$, they both agree with the passive line model. This has been confirmed by numerical modelling, and the agreement can be confirmed by inspection of equations (1) and (7).

Intuitively, it seems reasonable to investigate the rigid marker model more closely because, in ductile rocks, magnetite and hematite would be relatively rigid with respect to a limestone or soft sandstone matrix. Consequently, in Fig. 4 the passive line model is compared with the rigid model for different aspect ratios of the markers. For a reasonable selection of aspect ratios, $R = 1.2$, 2 and 5, there is relatively little difference between the final angular positions of the markers, given that the shortening strain should be <35% to produce homogeneously strained specimens in these triaxial tests. For the largest aspect ratio, R or $R_0 = 5$, it would not be possible to distinguish between the rigid marker and passive line models. This may be the case in samples involving hematite whose grains commonly have high aspect ratios.

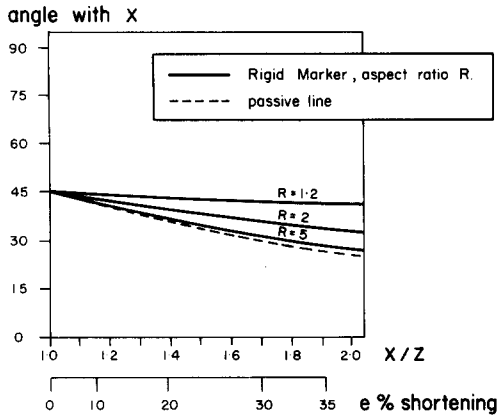

Fig. 4. The passive line model (Wettstein's equation, equation 1) compared with the rigid marker model (equation 7) for markers of differing ratio (R) of long axis/short axis. The shortening, e, refers to the shortening in the perfect flattening deformation used in this study ($X = Y > Z$).

TESTS OF THE THEORIES OF ROTATION WITH EXPERIMENTAL DATA

Several materials have been used to test the models for rotation of remanence. These include Ancaster limestone (Borradaile 1991), China Beach sandstone (Borradaile & Mothersill 1991) and synthetic aggregates of calcite and Portland cement with multidomainal magnetite (Jackson *et al.* in press) and with hematite (Borradaile in press). Figure 5 indicates that, from tests on the acquisition of isothermal remanence, most of the materials behave magnetically like pseudo-single-domain (PSD) magnetite, apart from the synthetic aggregates to which large PSD magnetite (Jackson *et al.* in press) or hematite pigment (<0.5 μm) (Borradaile in press) was added. Curie points were determined for the magnetic grains in some materials and hysteresis properties were determined for others, so that the magnetic mineralogy is well known, except for the case of the China Beach sandstone which does not saturate its remanence with the equipment available (Fig. 6). This suggests the presence of a coercive component such as hematite or goethite, although most of the remanent magnetization is carried by magnetite (Fig. 5). The artificial isothermal remanent magnetization (IRM) that was applied to these samples before deformation saturated all specimens except those bearing hematite. The maximum field available, 900 mT, was used in those cases to provide a magnetization that could be deformed experimentally.

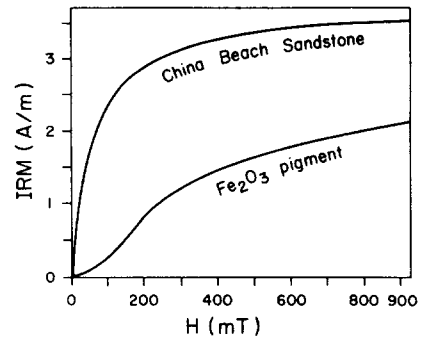

Fig. 6. The acquisition of IRM for two of the experimental materials carried to higher fields. Note the lack of saturation, indicating a high coercivity component in the China Beach sandstone.

Effects of strain on the intensity of remanence

Although we are primarily concerned with the effects of strain on the orientation of remanence, it is important to note that experimental deformation reduces the intensity of remanence (i.e. the length of the remanence vector). Figures 7(a) & (b) show this for some of the specimens. Many others have been deformed in which

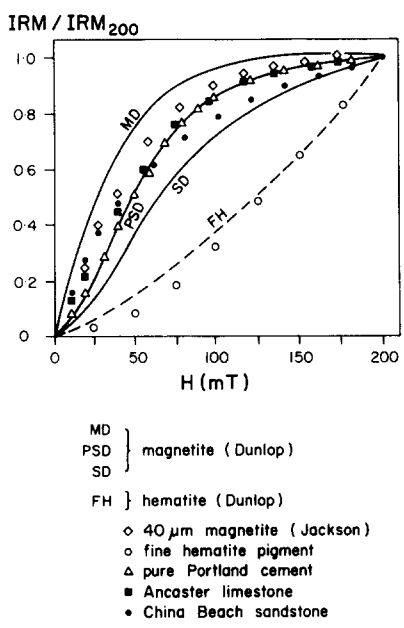

Fig. 5. The acquisition of isothermal remanent magnetization (IRM) for the experimentally deformed materials. The data are compared with the standard reference curves of Dunlop (1971, 1972, 1981, 1983).

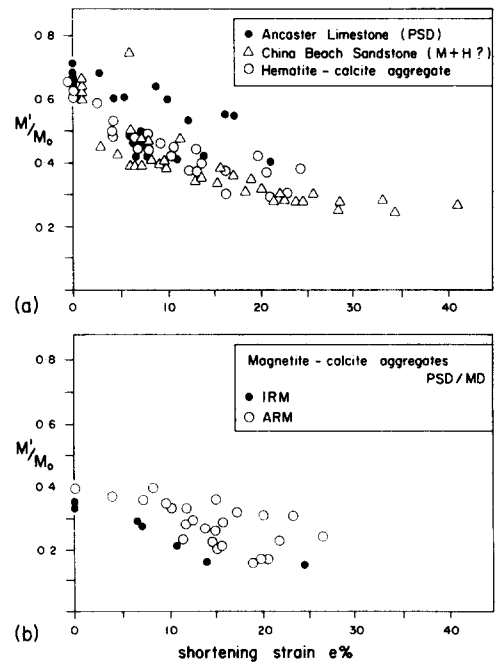

Fig. 7. The decrease in magnetization for experimentally deformed specimens. $e = 0$ refers to specimens that have been hydrostatically compacted.

there are two components of IRM applied in different directions; these are considered elsewhere (Borradaile 1992).

For the single-direction remanences in materials with relatively strong coercivities (Fig. 7a) we note that hydrostatic compaction alone ($e = 0$) reduces the intensity to about 65% of its initial value. Strain progressively reduces the intensities to about 30% of their initial value at a bulk shortening with a strain of 40%. The less coercive material (40 μm magnetite) shows even greater reductions in intensity (Fig. 7b). The anhysteretic remanence (ARM) of the magnetite studied by Jackson *et al.* (in press) was less reduced than the IRM in the same material studied by the author.

Pressure 'demagnetization' has been reported previously in connection with hydrostatic pressure (e.g. Pearce & Karson 1981, for a more recent study) or uncontrolled uniaxial deformation tests at negligible strains (see review by Nagata 1970). It should be remembered that even in hydrostatic tests, at the grain-scale, the magnetic grains are subjected to differential stresses although the macroscopic stresses are hydrostatic. This is expected of any polycrystalline material. The decrease in magnetization is clearly related to progressive triaxial strain (Figs. 7a & b). However, most of these tests involve increasing macroscopic differential stress. How can we distinguish the effects of finite strain from the effect of stress? Hydrostatic compaction tests may answer this. During hydrostatic tests the specimens are progressively compacted producing differential stresses at the microscopic, grain-scale. With the passage of time (Fig. 8) the effects of progressive grain damage are seen without any increases in differential stress. Thus the decreases in magnetization (Fig. 7) can probably be attributed to grain damage, including grain rotation which disperses the remanence directions of the grains and weakens the intensity of the bulk remanence vector.

The effects of strain are not felt uniformly by all the components of remanence. Components residing in magnetically 'softer' grains, i.e. grains of lower coercivity, are reduced in intensity more than components in higher coercivity grains, at least where magnetite is the dominant carrier or remanence. This is shown by comparing the coercivity spectra for the same samples before and after deformation (Fig. 9). The large components of remanence residing in grains of low coercivity (those removed by <20 mT peak a.f. demagnetization) are dramatically removed for the two examples shown.

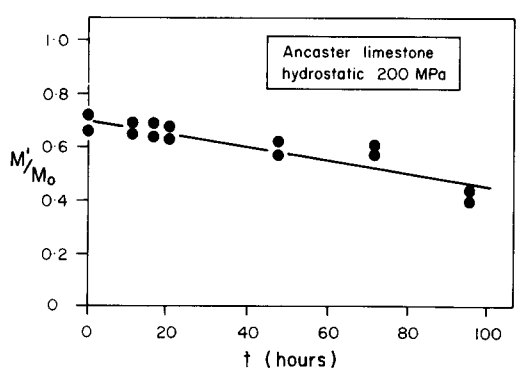

Fig. 8. Decrease of intensity of magnetization with time for specimens that have only been subjected to hydrostatic compaction.

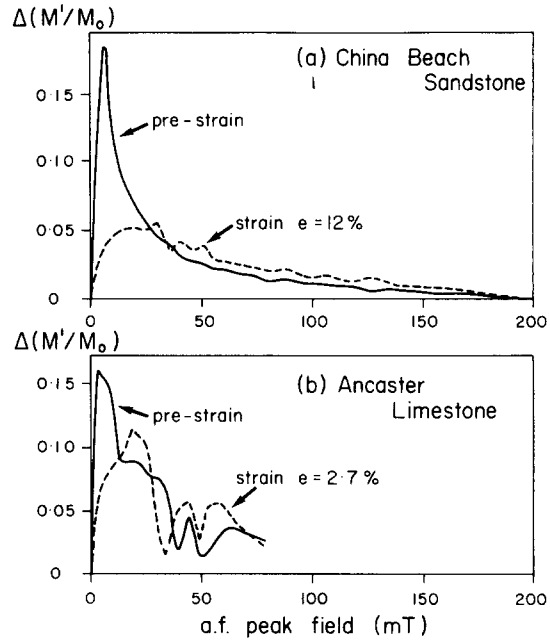

Fig. 9. Coercivity spectra of samples before and after triaxial deformation for the shortening strains indicated.

Effect of strain on the attitude of remanence

The samples carry a single direction of remanence imposed by a field that saturates the magnetic grains present, in most samples. It is discussed elsewhere that the effects of strain on a remanence composed of multi-directional components of different coercivity are quite different (Borradaile & Mothersill 1991, Borradaile 1992). Such is the situation when deformation affects a natural remanent magnetization (NRM). However, paleomagnetists are concerned mainly with the characteristic, primary component of remanence which is, of course, unidirectional. Thus the single direction IRM applied here should respond to strain in a way that will enable us to predict the response of the characteristic component of an NRM to natural deformation. In the experiments the IRM was imposed at different inclinations to the long axis of the cylindrical specimens so that the inclination corresponds to the initial angle θ of the theoretical section above, i.e. the angle between the remanence direction and the maximum extension direction.

The simplest comparison that can be made is of the ratio of tangents of the inclinations before (I_0) and after (I'_{exp}) strain with the actual experimental strain ratio (R_{exp}). Perfect agreement with the passive line model (equation 1) should then give a straight line of unit slope. The agreement is poor (Fig. 10), except perhaps in the case of the hematite–calcite aggregates. An estimated error of observation of ±2° in the orientation of inclination, gives rise to generous error bars, as shown in Fig.

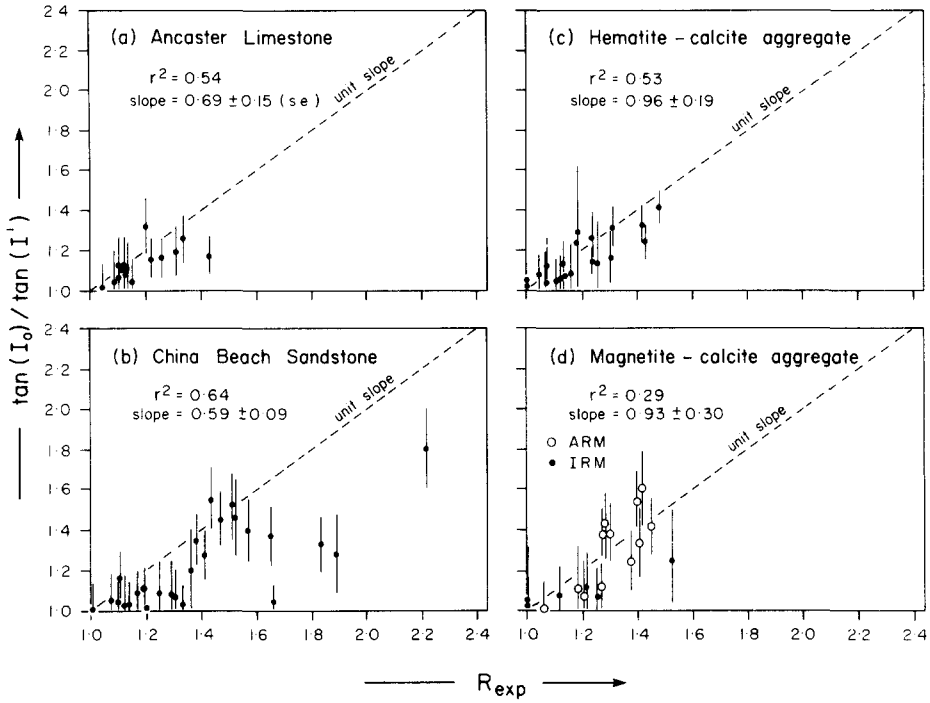

Fig. 10. Degree of agreement with the passive line model for the experimental data. If the results showed perfect agreement with equation (1), the points would all lie on a straight line of unit slope. The regression parameters (r^2) show that this agreement is poor, except perhaps in the case of the synthetic aggregates of hematite–calcite. The ARM data of (d) are from Jackson *et al.* (in press). Here $R_{exp} = Z^{-1.5}$, which assumes constant volume, simple flattening by shortening of the Z-axis. Anomalous behaviour for $R_{exp} < 1.2$ may be attributed to volume reduction early in the experiments as shown by Jackson *et al.* (in press).

10. These errors were based on partial derivatives of equation (1) (Topping 1955). Jackson *et al.* (in press) noted that at small strains the effects of volume reduction, early in the experimental deformation, produce some departures from ideal behaviour. This may be noted in Figs. 10(b) & (d), where, for $R_{exp} < 1.3$, there is almost no change in inclination. This would indicate that initial volume reduction is suppressing the effects of strain.

We may also compare the final inclinations of the remanences after deformation (I'_{exp}) with the inclinations that would have been expected if the remanence had behaved precisely as a passive line (I'_{theory}). Because the changes in angle are small this plot (Fig. 11) appears

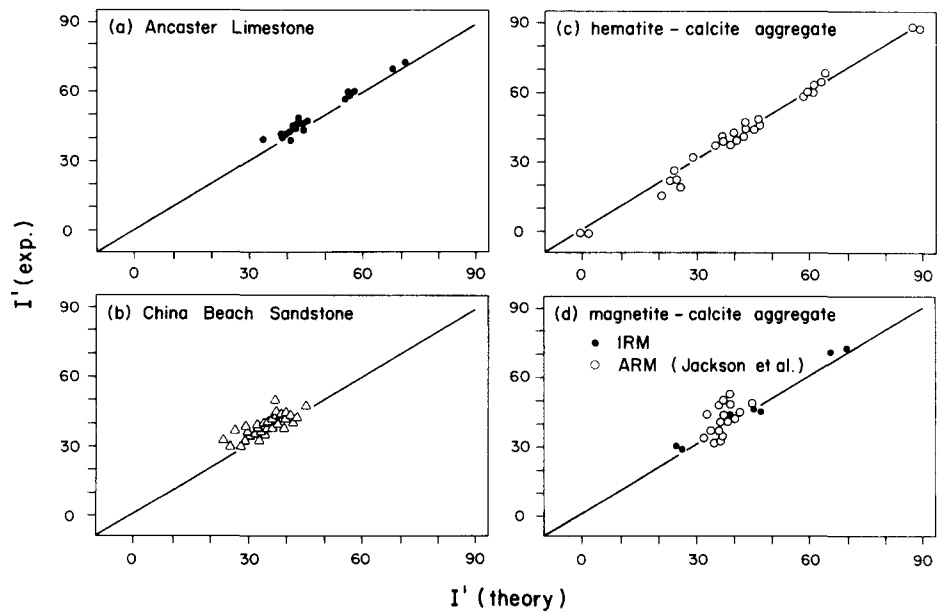

Fig. 11. The final inclinations of magnetic remanence after experimental deformation [I'_{exp}] plotted against the final inclinations [I'_{theory}] that would have been predicted by the passive line model. The differences are slight for the range of strains considered. The straight line is not a regression line: it is simply a line of unit slope that would indicate perfect agreement with equation (1).

superficially to give much better agreement with the passive line model than the plots shown in Fig. 10. It is useful, however, because we can inspect the sense of the deviation of the I'_{exp} values from the expected values. If the I'_{exp} values are too high, the rotation is less than a passive line and a rigid-marker model may be more appropriate. If the I'_{exp} values are too low, the rotation of the remanence is faster than a passive line and a passive elliptical marker model is more appropriate. In the graphs of Fig. 11, the straight line indicates a perfect passive linear model relationship.

First inspection of the graphs shows that in all cases the final orientations of the remanences lie close to the linear relationship predicted by the passive line model. Further inspection shows that in the case of the Ancaster limestone (Fig. 11a), China Beach sandstone (Fig. 11b) and synthetic magnetite–calcite aggregates (Fig. 11d) the data points all lie to the high side of the passive linear relationship. This indicates that their remanences rotated slightly too slowly to be accounted for by the passive line model. However, in the case of the hematite–calcite synthetic aggregate it is not possible to show that the data disagree with the passive line model.

DISCUSSION

The results of 121 triaxial deformation tests on artificially magnetised limestone, sandstone and mineral aggregates have been examined in this paper. The conditions of experimental deformation are not directly comparable to those in nature. Although the strain-rate (10^{-5} s^{-1}) is very constant, providing smooth stress–strain relations (Fig. 1) and macroscopically ductile deformation, it is about 10^6 times faster than a geological strain-rate for regional deformation. Consequently, the flow stresses (Fig. 1) are approximately two orders of magnitude higher than those in nature (Raleigh & Evernden 1981, Carter & Tsenn 1987). High stresses in experiments would be expected to introduce more dislocations in remanence-bearing crystals and thus impede the motion of domain walls associated with *intragranular* rotation of remanence. However, in this study, and in field studies, it has been assumed that the remanence rotates solely due to the spinning of the grain in the rock matrix. The results of the experiments are equivocal (Fig. 10). Nevertheless, it has been pointed out that for the range of shortening capable of producing homogeneously strained specimens in these experiments, only small differences are to be expected for the final angles predicted by the three different models (Fig. 3). This is borne out by Fig. 11 which indicates that, whatever the mechanism of deformation, the differences between it and the passive model have little practical consequence for the present range of strains.

The small departures from the passive line model, particularly shown in Figs. 11(a), (b) & (d) indicate that inclinations of remanence are too high or that rotation is too small for the passive line model. This evidence lends support to the rigid marker model.

Table 1. Effective grain aspect ratios calculated from remanence rotation

	R	Standard deviation
Ancaster limestone	2.022	1.509
China Beach sandstone	1.675	1.179
Aggregate with magnetite	1.480	0.908
Aggregate with hematite	4.304	1.632

In order to test the reality of the rigid marker model, the effective mean aspect ratio R has been calculated for each experiment by rearranging equation (7). The mean values of R that would explain the rotation by a perfect rigid marker value are given in Table 1.

The results indicate that the effective mean particle aspect ratios for the Ancaster limestone, China Beach sandstone and synthetic magnetite lie between 1.4809 and 2.022. These are reasonable values for magnetite grains in these materials. For such values of R, small differences between the rigid marker and passive marker model are expected (see Fig. 4) and these are confirmed by experiment (Figs. 11a, b & d). In the case of the synthetic hematite aggregate, it is barely possible to distinguish the actual deformation process from the passive model (Fig. 11c). However, the rigid model would be compatible with a grain aspect ratio $R = 4.304$ (Table 1) which is quite close to the ratios of these synthetic hematite flakes when observed by scanning electron microscope. Inspection of Fig. 4 shows that at the low strains achieved, one could not expect to distinguish the rigid and passive models in this case.

In conclusion, it appears that where magnetite carries the remanence in these experiments, the remanence vector does not appear to rotate as a passive line (Fig. 10) and it may rotate as a rigid marker. However, for the strains involved (0–35% shortening), the differences from the passive model are slight and Wettstein's equation (equation 1), or its three-dimensional equivalent (in this study, equation 2 as $X = Y > Z$) may be used to restore the final remanence attitude to its pre-deformation attitude (Fig. 11). In the case of a remanence carried by hematite, the rotation of the grains and the remanence is indistinguishable from the passive line model at these strains (and still higher strains) because of the large R value for hematite flakes. This may explain the success of equation (1) in restoring remanence directions for large finite strains from naturally deformed red-beds (e.g. Kligfield *et al.* 1981, 1983, Cogné & Perroud 1985, Hirt *et al.* 1986, Cogné 1987a). In this, as most other studies, it has been assumed that the strain history is coaxial. In more complex non-coaxial strain histories such as simple shear or combinations of pure shear and simple shear, the relative rates of rotation of rigid and passive line markers are more complex and not always intuitively predictable (Ghosh & Ramberg 1976). The interpretation of remanence rotation under those circumstances may be more difficult than has hitherto been appreciated (e.g. Kodama & Goldstein 1991, Stamatakos & Kodama 1991a,b). Nevertheless, under some circumstances, it may be

easier to distinguish between the different theoretical models of remanence rotation in non-coaxial strain histories.

Acknowledgements—I would like to thank John Ramsay for permitting me to audit his very stimulating M.Sc. course at Imperial College in the winter of 1969–1970. I feel very fortunate to have been one of the recipients of his superb and enthusiastic teaching. I thank John also on behalf of my students and myself for his masterly publications that have advanced structural geology greatly as a distinct scientific discipline.

This work was supported by the Natural Sciences and Engineering and Research Council of Canada (NSERC). The writer is grateful for the support of NSERC and BILD in establishing a rock physics laboratory. I thank Pierre Rochette for helpful correspondence which provoked improvements to this manuscript, Anne Hammond for excellent specimen preparation and Sam Spivak for drafting. Mike Jackson and Ben van der Pluijm provided constructively critical reviews.

REFERENCES

Borradaile, G. J. 1991. Remanent magnetism and ductile deformation in an experimentally deformed magnetite-bearing limestone. *Phys. Earth & Planet. Interiors* **67**, 362–373.

Borradaile, G. J. 1992. Experimental deformation of two-component IRM in magnetite-bearing limestone: a model for the behaviour of NRM during natural deformation. *Phys. Earth & Planet. Interiors* **70**, 64–77.

Borradaile, G. J. In press. Deformation of remanent magnetism in a synthetic aggregate with hematite. *Tectonophysics*.

Borradaile, G. J. & Mothersill, J. S. 1989 Tectonic strain and paleomagnetism: experimental investigation. *Phys. Earth & Planet. Interiors* **56**, 254–265.

Borradaile, G. J. & Mothersill, J. S. 1991. Experimental strain of isothermal remanent magnetisation in ductile sandstone. *Phys. Earth & Planet. Interiors* **65**, 308–318.

Carter, N. L. & Tsenn, M. C. 1987. Flow properties of continental lithosphere. *Tectonophysics* **136**, 27–63.

Cogné, J.-P. 1987a. Paleomagnetic direction obtained by strain removal in the Pyrenean Permian redbeds at the "Col du Somport" (France). *Earth Planet. Sci. Lett.* **85**, 162–172.

Cogné, J.-P. 1987b. Experimental and numerical modelling of IRM rotation in deformed synthetic samples. *Earth Planet Sci. Lett.* **86**, 39–45.

Cogné, J.-P. 1988. Strain, magnetic fabric, and paleomagnetism of the deformed red beds of the Pont-Rean Formation, Brittany, France. *J. geophys. Res.* **93**, 13,673–13,687.

Cogné, J.-P. & Gapais, D. 1986. Passive rotation of hematite during deformation: a comparison of simulated and natural redbeds fabrics. *Tectonophysics* **121**, 365–372.

Cogné, J.-P. & Perroud, H. 1985. Strain removal applied to paleomagnetic directions in an orogenic belt: the Permian red slates of the Alpes Maritimes, France. *Earth Planet. Sci. Lett.* **72**, 125–140.

Cogné, J.-P. & Perroud, H. 1987. Unstraining paleomagnetic vectors: the current state of debate. *Eos* **68**, 705–712.

Dunlop, D. J. 1971. Magnetic properties of fine particle hematite. *Annls Geophys.* **27**, 269–293.

Dunlop, D. J. 1972. Magnetite: behaviour near the single-domain threshold. *Science* **176**, 41–43.

Dunlop, D. J. 1981. The rock magnetism of fine particles. *Phys. Earth & Planet. Interiors* **26**, 1–26.

Dunlop, D. J. 1983. Determination of domain structure in igneous rocks by alternating field and other methods. *Earth Planet. Sci. Lett.* **63**, 353–367.

Ghosh, S. K. & Ramberg, H. 1976. Reorientation of inclusions by combination of pure shear and simple shear. *Tectonophysics* **34**, 1–70.

Hirt, A. M., Lowrie, W. & Pfiffner, O. A. 1986. A paleomagnetic study of tectonically deformed red beds of the Lower Glarus Nappe Complex, Eastern Switzerland. *Tectonics* **5**, 723–731.

Jackson, M., Borradaile, G. J., Hudleston, P. J. & Banerjee, S. K. In press. Experimental deformation of synthetic magnetite-bearing calcite sandstones: effects on remanence, bulk magnetic properties and magnetic anisotropy. *J. geophys. Res.*

Kligfield, R., Lowrie, W., Hirt, A. & Siddans, A. W. B. 1983. Effect of progressive deformation on remanent magnetization of Permian Redbeds from the Alpes Maritimes (France). *Tectonophysics* **97**, 59–85.

Kligfield, R., Owens, W. H. & Lowrie, W. 1981. Magnetic susceptibility anisotropy, strain and progressive deformation in Permian sediments from the Maritime Alps (France). *Earth Planet. Sci. Lett.* **55**, 181–189.

Kodama, K. P. 1988. Remanence rotation due to rock strain and the stepwise application of the fold test. *J. geophys. Res.* **93**, 3357–3371.

Kodama, K. P. & Cox, A. 1978. The effects of a constant volume deformation on the magnetisation of an artificial sediment. *Earth Planet. Sci. Lett.* **38**, 436–442.

Kodama, K. P. & Goldstein, A. G. 1991. Experimental simple shear deformation of magnetic remanence. *Earth Planet. Sci. Lett.* **104**, 80–85.

Lowrie, W., Hirt, A. M. & Kligfield, R. 1986. Effects of tectonic deformation on the remanent magnetization of rocks. *Tectonics* **5**, 713–722.

MacDonald, D. W. 1980. Net tectonic rotation, apparent tectonic rotation and the structural tilt correction in paleomagnetic studies. *J. geophys. Res.* **85**, 3659–3669.

Nagata, T. 1970. Basic magnetic properties of rocks under the effects of mechanical stresses. *Tectonophysics* **9**, 167–195.

Pearce, G. W. & Karson, J. A. 1981. On pressure demagnetisation. *Geophys. Res. Lett.* **8**, 725–728.

Pfiffner, O. A. & Ramsay, J. G. 1982. Constraints on geological strain-rates: arguments from finite strain states of naturally deformed rocks. *J. geophys. Res.* **87**, 311–321.

Pozzi, J.-P. & Aïfa, T. 1989. Effects of experimental deformation on the remanent magnetization of sediments. *Phys. Earth & Planet. Interiors* **58**, 255–26.

Raleigh, B. & Evernden, J. 1981. The case for low deviatoric stress in the lithosphere. In: *Mechanical Behaviour of Crustal Rocks* (edited by Carter, N. L., Friedman, M., Logan, J. M. & Stearns, D. W.). *Am. Geophys. Un. Geophys. Monogr.* **24**, 173–186.

Ramsay, J. G. 1967. *Folding and Fracturing of Rocks*. McGraw-Hill, New York.

Ramsay, J. G. & Huber, M. I. 1983. *The Techniques of Modern Structural Geology, Volume* 1: *Strain Analysis*. Academic Press, London.

Rosenbaum, J. G. 1986. Paleomagnetic directional dispersion produced by plastic deformation in a thick Miocene welded tuff, southern Nevada: implications for welding temperatures. *J. geophys. Res.* **91**, 12,817–12,834.

Stamatakos, J. & Kodama, K. P. 1991a. Flexural flow folding and the paleomagnetic fold test: an example of strain reorientation of remanence in the Mauch Chunk Formation. *Tectonics* **10**, 807–819.

Stamatakos, J. & Kodama, K. P. 1991b. The effects of grain-scale deformation on the Bloomsburg formation pole. *J. geophys. Res.* **96**, 17,919–17,933.

Tarling, D. H. 1974. A paleomagnetic study of Eocambrian tillites in Scotland. *J. geol. Soc. Lond.* **130**, 163–177.

Topping, J. 1955. *Errors of Observation and Their Treatment*. Chapman & Hall, London.

van der Pluijm, B. A. 1987. Grain-scale deformation and the fold test—evaluation of syn-folding remagnetization. *Geophys. Res. Lett.* **14**, 155–157.